

In situ XAFS study on cathode materials for lithium-ion batteries

Takamasa Nonaka,^a Chikaaki Okuda,^a Yoshio Ukyo^a and Tokuhiko Okamoto^a

^aTOYOTA Central Research & Development Laboratories., Inc., Nagakute, Aichi, 480-1192, Japan
Email:nonaka@mosk.tytlabs.co.jp

Ni and Co K-edge X-ray absorption spectra of $\text{LiNi}_{0.8}\text{Co}_{0.2}\text{O}_2$ have been collected using *in situ* coin cells. To investigate the electronic and structural changes accompanied by the capacity fading during electrochemical cycling and keeping batteries at high temperatures, the cells with different cycling states and keeping conditions (temperature, time) were prepared. Upon charging the cell, the Ni and Co K absorption edge shifted towards higher energy, and the good correlation between the range of chemical shifts upon charging and the capacity of the cell was observed. From quantitative analysis of EXAFS data, it was revealed that the capacity fading is closely related to the Jahn-Teller distortion of the NiO_6 octahedron.

Keywords: rechargeable battery, cathode, nickel, cobalt, *in situ* measurement.

1. Introduction

$\text{LiNi}_{0.8}\text{Co}_{0.2}\text{O}_2$ is one of the current candidates for a cathode material of advanced rechargeable batteries with high capacity. It is known that the stability of $\text{LiNi}_{0.8}\text{Co}_{0.2}\text{O}_2$ is superior to that of LiNiO_2 because of exhibiting a single-phase region upon oxidation from 3.0V to 4.1V (Levi *et al.*, 1999). However, the capacity fading occurs not only during charge/discharge cycling but also when batteries are kept at high temperatures. And this capacity fading is most important problem for practical use. From the standpoint of overcoming the capacity fading, it is essential to understand the electronic and structural changes accompanied by the capacity fading. For this purpose, *in situ* XAFS analysis is very useful, because it will give the information on the local structure around an absorber atom and its electronic structure without destructing the battery for a measurement. Some studies applying *in situ* XAFS analysis for LiNiO_2 or LiCoO_2 have been already reported (Mansour *et al.*, 1999, Nakai *et al.*, 1997). But an *in situ* XAFS study on the capacity faded battery has not been reported yet. So we prepared the batteries with various capacities and have measured *in situ* Ni and Co K-edge absorption spectra of $\text{LiNi}_{0.8}\text{Co}_{0.2}\text{O}_2$.

2. Experimental

2.1 Sample preparation

Figure 1 shows a drawing of the coin cell newly developed for *in situ* XAFS measurements in a transmission mode. By using 0.4 mm Beryllium windows, the X-rays can penetrate through the cell. XAFS data can be obtained at various voltages without taking out the cathode material from the cell.

To investigate the changes resulting from cycling and keeping at high temperatures, the cells with different cycling states and keeping conditions (temperature, time) were prepared. The cells used in this study are listed in Table 1.

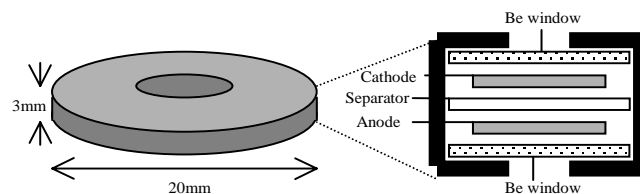


Figure 1
Schematic drawing of the *in situ* coin cell.

Table 1
The conditions of cells

Cell no.	Condition	Capacity (relative value)
1	Initial state (no treatment)	NA
2	After one charge/discharge cycle*	100
3	After 515 charge/discharge cycles*	9.5
4	After keeping at 80°C for 3 days**	64.3
5	After keeping at 60°C for 25 days**	14.7

* The charge/discharge cycling have been done at rate of $1\text{mA}/\text{cm}^2$ in the range of voltage from 3.0V to 4.1V. ** Kept at charged state which corresponds to a voltage of 4.1V.

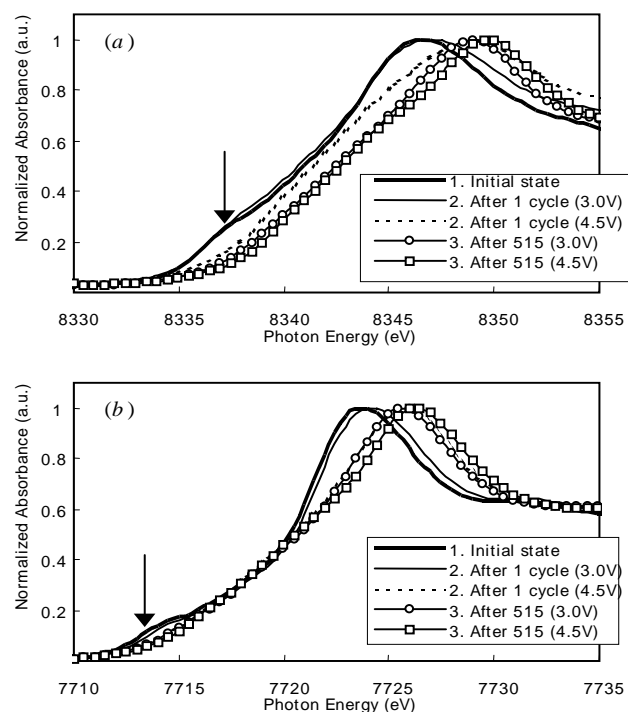


Figure 2
(a) Ni K-edge and (b) Co K-edge XANES spectra of $\text{LiNi}_{0.8}\text{Co}_{0.2}\text{O}_2$.

2.2 XAFS measurements

Ni and Co K-edge XAFS data were collected using beamline BL16B2 in SPring-8 (Hyogo, Japan). The incident X-rays were monochromatized using Si (111) double-crystal monochromator, and the harmonic content of the beam was minimized by Rh-coated Si mirror inclined to 5 mrad. The X-ray intensities were monitored using ionization chambers filled with nitrogen gas for the incident beam and a mixture of argon (25%) and nitrogen (75%) for the transmitted beam.

3. Results and Discussion

3.1 XANES

Figures 2 (a) and (b) show the Ni K-edge and Co K-edge XANES spectra of $\text{LiNi}_{0.8}\text{Co}_{0.2}\text{O}_2$ for several samples. In both edges, chemical shifts of the edge peak energy were found. And it should be noticed that some structures were observed in the energy region 8335-8340 eV (indicated by arrows in the figures), which are discussed later.

The graphical comparisons of the edge peak energies as a function of the cell voltages are shown in Figures 3 (a) and (b). The edge peak energy E_p is defined here as the energy at maximum height of the edge jump. Continuous shifts toward higher energies are thought to indicate the increases in the average oxidation states of Ni upon lithium removal (Nakai *et al.*, 1997). In capacity faded samples, the ranges of chemical shifts upon charging are less than that in "After one cycle". A good correlation between the range of chemical shift and the capacity of the cell was found. It is also worth noticing that the chemical shifts of Co and Ni K-edge occur in the same way in spite of difference of the electronic structure between Ni and Co. The reason for this phenomenon is not clear now.

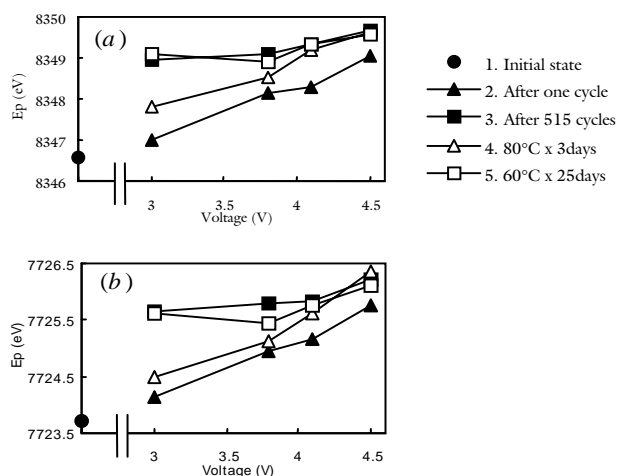


Figure 3
Graphical comparisons of the edge peak energies (E_p) as a function of the voltages for (a) Ni K-edge and (b) Co K-edge.

3.2 EXAFS

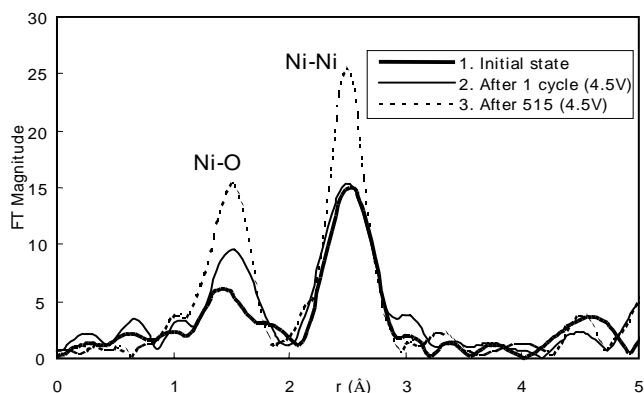


Figure 4
Fourier-transforms of Ni K-EXAFS spectra for $\text{LiNi}_{0.8}\text{Co}_{0.2}\text{O}_2$.

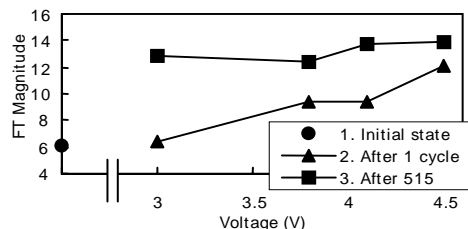


Figure 5
A comparison of the heights of Ni-O peaks in FT spectra as a function of the voltages.

Fourier-transforms of the Ni K-edge EXAFS spectra for several samples are shown in Fig. 4. The first peak at around 1.5\AA corresponds to Ni-O interactions and the second one at around 2.5\AA corresponds to Ni-Ni interactions. The Ni-O peak height of the sample in its initial state is lower than that of capacity faded samples. This phenomenon is explained by the local Jahn-Teller distortion of the NiO_6 octahedron due to the low spin Ni^{3+} . Distorted NiO_6 octahedral coordination such as 4(shorter)+2(longer) Ni-O bonds causes the apparent decrease in the height of the Ni-O peak due to the interference of imaginary and real part of the FT (Nakai *et al.*, 1997). Fig. 5 shows the heights of the Ni-O peak as a function of the cell voltage. Upon charging, the extent of the local distortion is getting lower, and the distorted NiO_6 octahedron turns into a regular octahedron. This phenomenon is resulting from gradual changes of the average valence of Ni from 3+ to 4+; therefore, the shape of Fig. 5 is very similar to that of Fig. 3 (a).

The averages of the Ni-O distances deduced from quantitative analysis of EXAFS data are shown in Fig. 7. The curve-fitting were performed with the coordination numbers of oxygen fixed to 6. The phase shifts and backscattering amplitudes were obtained from the tabulated functions calculated by McKale *et al.* (McKale *et al.*, 1988).

In "After one cycle", the Ni-O distance obviously decreases upon charging, while in "After 515 cycles", the distance changes only slightly. It is supposed that the change of the Ni-O distance is originating mainly from the change of the ion-radii accompanied by the oxidation of Ni^{3+} to Ni^{4+} .

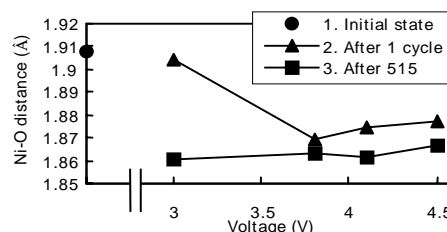


Figure 6
A comparison of the averages of Ni-O distances as a function of the voltages.

3.3 Molecular orbital calculations for XANES spectra

To assign the structures that were observed in the energy region 8335-8340 eV of XANES spectra, first-principles molecular orbital calculations were performed using the discrete variational (DV) $X\alpha$ cluster method (Ellis *et al.*, 1976). Fig. 7 (a) shows a model cluster used in the present calculations. To investigate the effect of the local distortion of NiO_6 octahedron, the model cluster with a regular octahedron and the one with a distorted octahedron (4 shorter Ni-O and 2 longer Ni-O) were used for comparison. In this work, a program code SCAT

(Adachi *et al.*, 1978) was used to calculate the electronic states of the model clusters. The atomic orbitals used in the calculations are $1s-4p$ for Ni, and $1s-3p$ for O.

XANES spectra reproduced by the calculations are shown in Fig. 7 (b). The absorption intensity at around 8337 eV in the calculated spectrum with distorted octahedron was larger than that with regular octahedron. From these calculations, it is suggested that the observed structures are originating from the local Jahn-Teller distortion of the NiO_6 octahedron.

As shown in Fig. 3 (b), the similar structures were found in Co K-edge XANES spectra. But, at present, we have no idea about these structures.

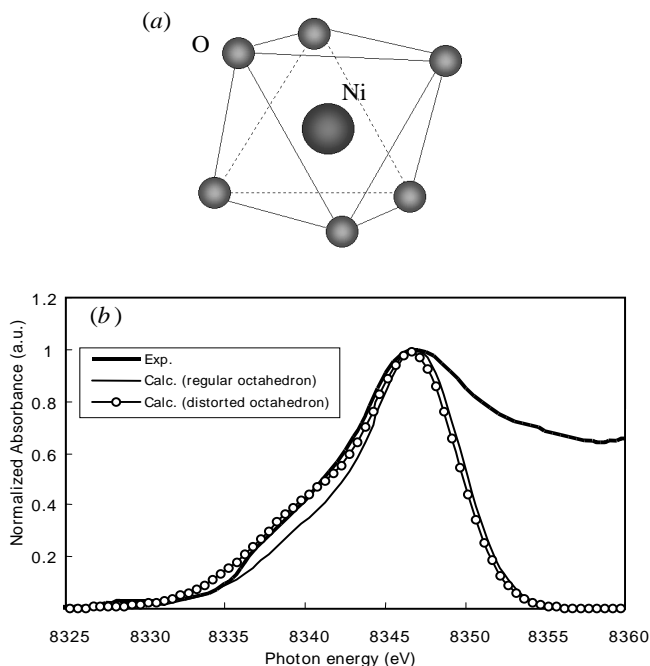


Figure 7
(a) The model cluster used for calculations, (b) A comparison of experimental and calculated Ni K-edge XANES spectra.

References

- Levi, E., Levi, M.D., Salitra, G., Aurbach, D., Oesten, R., Heider, U. & Heider, L. (1999). *Solid State Ionics* **126**, 97-108.
- Mansour, A.N., McBreen, J., Melendres, C.A. (1999). *J. Electrochemical Society* **146**(8), 2799-2809.
- Nakai, I., Takahashi, K., Shiraiishi, Y., Nakagome, T., Izumi, F., Ishii, Y., Nishikawa, F. & Konishi, T. (1997). *J. Power Sources* **68**, 536-539.
- McKale, A.G., Veal, B.W., Paulikas, A.P., Chan, S.K. & Knapp, G.S. (1988). *J. American Chemical Society* **110**, 3763.
- Ellis, D.E., Adachi, H. & Averill, F.W. (1976). *Surface Science* **58**, 497.
- Adachi, H., Tsukada, M. & Satoko, C. (1978). *J. Physical Society of Japan* **45**, 497.